

PROGRESS REVIEW

Reduction of non-fill defects in nanoimprint lithography

To cite this article: Toshiki Ito et al 2024 Jpn. J. Appl. Phys. 63 050804

View the article online for updates and enhancements.

You may also like

- <u>Bubble Manipulation by Self Organization of Bubbles inside Ultrasonic Wave</u>
 Yoshiki Yamakoshi and Masato
 Koganezawa
- <u>Highly Efficient Preconcentration of Per-</u> and Polyfluoroalkyl Substances (PFAS) by Anodically Generated Shrinking Gas Bubbles

Ruchiranga Ranaweera and Long Luo

- Effectiveness of air entraining agent and defoamer on the bubble distribution of fresh mortar under different mixing methods

Jianwei Hu, Yongjiang Xie, Zike Liu et al.

Check for updates

Reduction of non-fill defects in nanoimprint lithography

Toshiki Ito1*, Wei Zhang2, and Weijun Liu2

¹Canon Inc., 20-2 Kiyohara-Kogyodanchi, UtSunomiya-shi, Tochigi 321-3292, Japan

²Canon Nanotechnologies Inc., 1807 West Braker Lane, Bldg. C-300, Austin, TX 78758, United States of America

*E-mail: ito.toshiki@mail.canor

Received December 21, 2023; revised March 3, 2024; accepted March 26, 2024; published online May 20, 2024

Field-by-field-type UV nanoimprint lithography equipped with an on-demand inkjet dispense system, known as jet and flash imprint lithography (JFIL), has been developed. In JFIL, the inkjet resist drops still remain independent of each other when imprinting a mold, so that the ambient gas is trapped among the resist drops to generate bubbles. It takes time for the trapped bubbles to disappear, and the bubbles sometimes remain in the cured resist film to cause open defects. The waiting time for the disappearance of the gas results in low throughput and the remaining bubbles cause defect problems in JFIL. The fast disappearance of trapped bubbles was demonstrated in the case when carbon dioxide gas was used as the ambient gas. On the basis of fluid mechanics, combined-drop JFIL and its resist material was developed, in which the resist drops were combined with each other prior to imprinting to minimize trapped gas volume. © 2024 The Japan Society of Applied Physics

1. Introduction

1.1. Jet and flash imprint lithography

Nanoimprint lithography (NIL) has been proposed as an effective technique for the replication of nanoscale features. ^{1,2)} Jet and flash imprint lithography (JFIL) involves the field-by-field deposition and exposure of a low viscosity resist deposited by jetting technology onto a substrate. Canon considers JFIL technology the best method for semiconductor device manufacturing ^{3–21)} due to its advantage in overlay.

The JFIL process is schematically depicted in Fig. 1. When compared to other imprint techniques, JFIL differentiates itself in its ability to adjust to pattern density variations as a result of using an inkjet dispensing method, as opposed to a more conventional spin-coat-based process. Resist volume is adjusted relative to the pattern density of the mold, thereby creating residual layers that are uniform across the patterned area. Because the resist volume deposited is matched to the mold pattern density, there is no wasted resist, and the resulting total volume of resist liquid dispensed on a substrate is around 0.001 times smaller than a spin-coat-type resist.

After the resist is dispensed, the patterned mold is lowered into the fluid, which then quickly flows into the relief patterns in the mold by capillary action, during which alignment is concurrently performed. Following this filling step, the resist is cured and cross-linked under UV radiation, the mold is removed, and a patterned resist is left on the substrate.

All the steps described above are carried out repeatedly on one wafer as a step-and-repeat process to fabricate nanoscale features on the whole wafer.

When compared to spin-coat-type imprint technology, JFIL has an advantage of uniformity of the residual layer thickness, since JFIL can adjust the resist volume in accordance with the variation of pattern density.

1.2. Resolution of JFIL technology

Our previous study¹³⁾ has demonstrated the resolution capability down to a half pitch 11 nm line and space (hp 11 nm l S⁻¹) and 10 nm pillar array (Fig. 2), which enables JFIL technology to be expanded to several nodes of technology.

JFIL has other differentiators from other types of lithography to fabricate complicated two-dimensional (2D) patterns (Fig. 3) and, furthermore, multi-step three-dimensional patterns such as a Dual Damascene structure.²²⁾

1.3. Challenges in JFIL

In JFIL, the close contact of the mold with the resist liquid causes various interactions, including pattern defects. The manufacturing yield of a semiconductor device is reduced by the defectivity; the number of defects should be decreased as much as possible. The defects caused in JFIL can be categorized as shown in Fig. 4.

In this paper, our effort to reduce imprint defects, especially non-fill defects, is reported.

2. Defect reduction

2.1. Ambient gas

A resist liquid is discretely dispensed into the pattern-forming field on the substrate, and the resist drops are still discrete when imprinting. Therefore, the ambient gas is trapped among the resist, the substrate, and the mold. The trapped ambient gas diffuses into the mold, the resist, and the substrate and finally disappears during imprinting time, but it takes a few tens of seconds in the case that the ambient gas is air atmosphere. The waiting time for gas disappearance results in low throughput and the remaining bubbles cause defect problems in JFIL.²³⁾

The resist drops spread to the whole field of the gap between the substrate and the mold by capillary force. This phenomenon is called spreading. The spreading process is classified into dynamic spreading (DS), which occurs after the mold surface contacts the resist droplets until the droplets of the resist combine with each other, and static spreading (SS), which occurs after the bonding and the trapped gas disappears. DS and SS can be observed through a quartz mold using an optical microscope (Fig. 5).

Some experimental results showed that DS completes within a few tens of milliseconds, while SS requires a few tens of seconds in the case of air atmosphere.²⁴⁾

Efforts have been made to quickly eliminate the trapped gas by using helium gas, which is easily diffused into the mold, ²⁴⁾ or carbon dioxide gas, which is easily dissolved into the resist of organic liquid, ²⁵⁾ as the ambient gases. The permeability coefficients of various gas molecules are summarized in Fig. 6.

The pore size of the lattice spacing of the mold material, quartz, is 100~300 pm, while the dynamic diameter of a helium atom is said to be 260 pm. Therefore, helium can

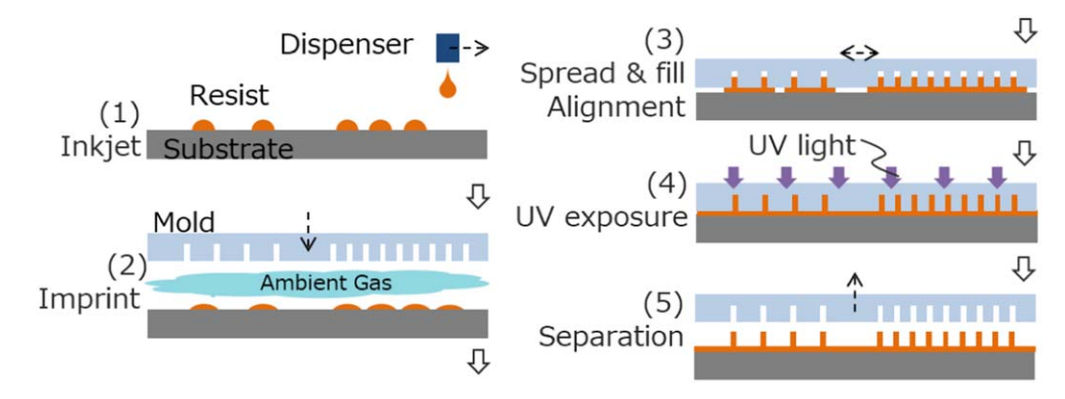


Fig. 1. The JFIL process.

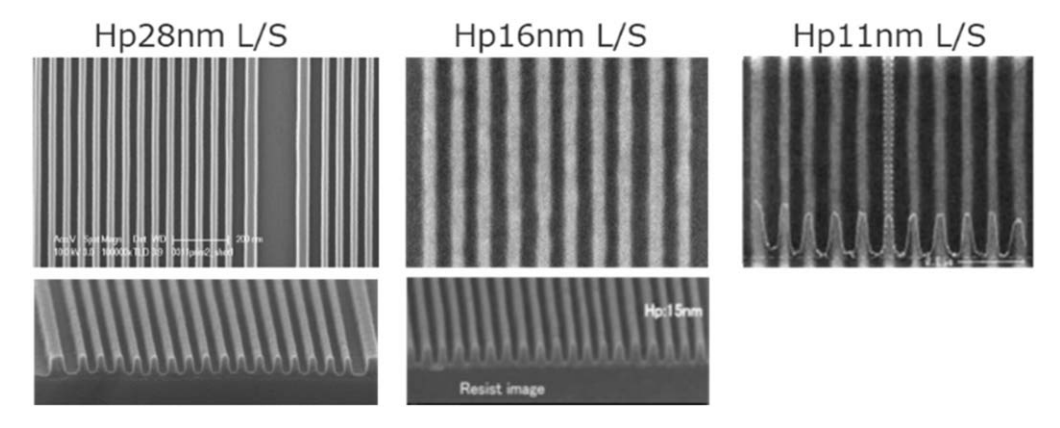


Fig. 2. Scanning electron microscope images of JFIL resist patterns.

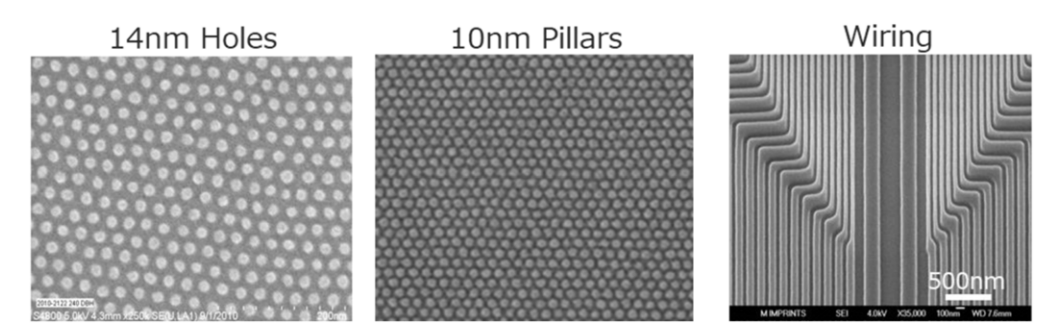


Fig. 3. Two-dimensional patterns fabricated by JFIL.

diffuse into a quartz mold. In the case of JFIL with helium as the ambient gas, trapped helium gas bubbles disappear quickly.²⁷⁾ Molecules of nitrogen, oxygen, and carbon dioxide are larger than 300 pm, so they cannot diffuse into a quartz mold.

However, it is well known that CO₂ gas has higher solubility into organic materials than helium, nitrogen, and oxygen. We hypothesize whether the trapped CO₂ gas bubbles can dissolve into the resist material or some kinds of organic substrate layers.

2.1.1. Calculation. In order to theoretically calculate the time required for DS and SS, a simplified model of the JFIL process was devised, as shown in Fig. 7.

The mold assumes a blank mold with no recess pattern formed. The resist drops dispensed onto the substrate in a square arrangement are independent of each other before the mold is contacted. When the mold is contacted, the mold surface is brought into contact with the resist, and DS starts. The resist drop is assumed to have a cylindrical shape and to

spread while maintaining a cylindrical shape. It is defined that DS is completed and SS starts at the moment when the resist drops contact each other. In SS, the ambient gas is trapped by the resist, the mold, and the substrate.

The unit cell of the square array in the SS process is approximated to a cylindrical coordinate system model, as shown in Fig. 7. The same volume of gas and resist as the unit cell of the Cartesian coordinate system is sandwiched between the disk-shaped substrate and the mold in the cylindrical coordinate system. The outer boundary of the disk is a closed boundary. Trapped ambient gas disappears by diffusion and dissolution with Laplace pressure as the driving force. If the resist is assumed to be an incompressible fluid, the mold descends to compensate for the volume of the missing gas. When the volume of the gas becomes zero, SS completion is defined. A droplet volume of 1 pL and drop diameter of $100~\mu m$ at the start of DS and a resist liquid film thickness of 20~nm at the end of SS were assumed.

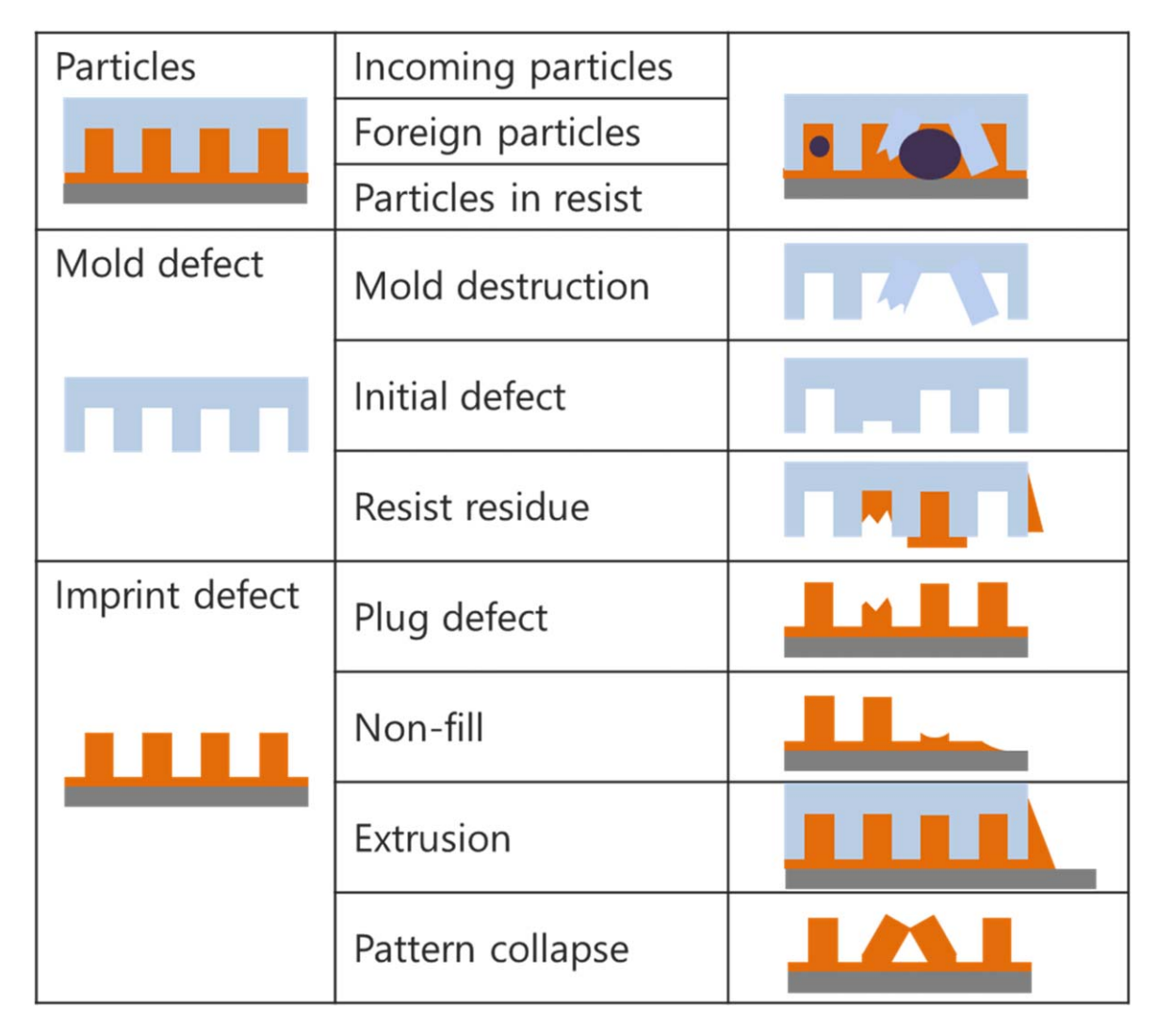


Fig. 4. Defect categories.

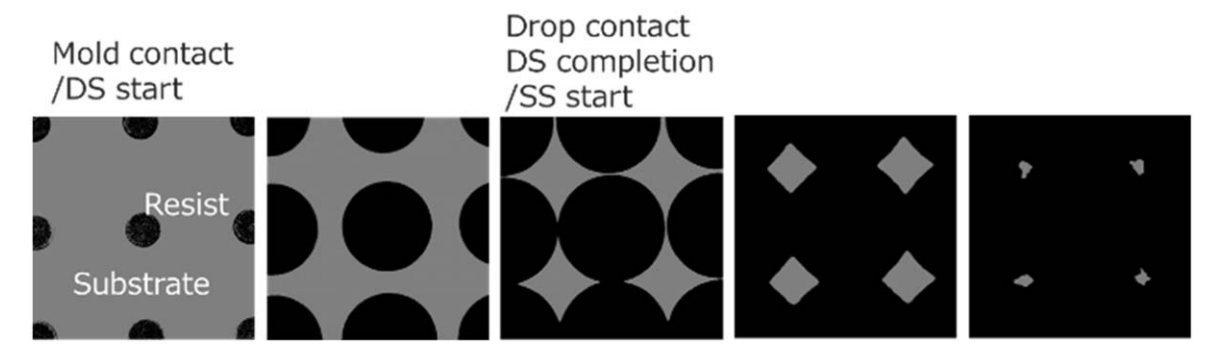


Fig. 5. Dynamic spread and static spread observed through a quartz mold.



Fig. 6. Permeability coefficients (kg/m•atm•s) of gas molecules.

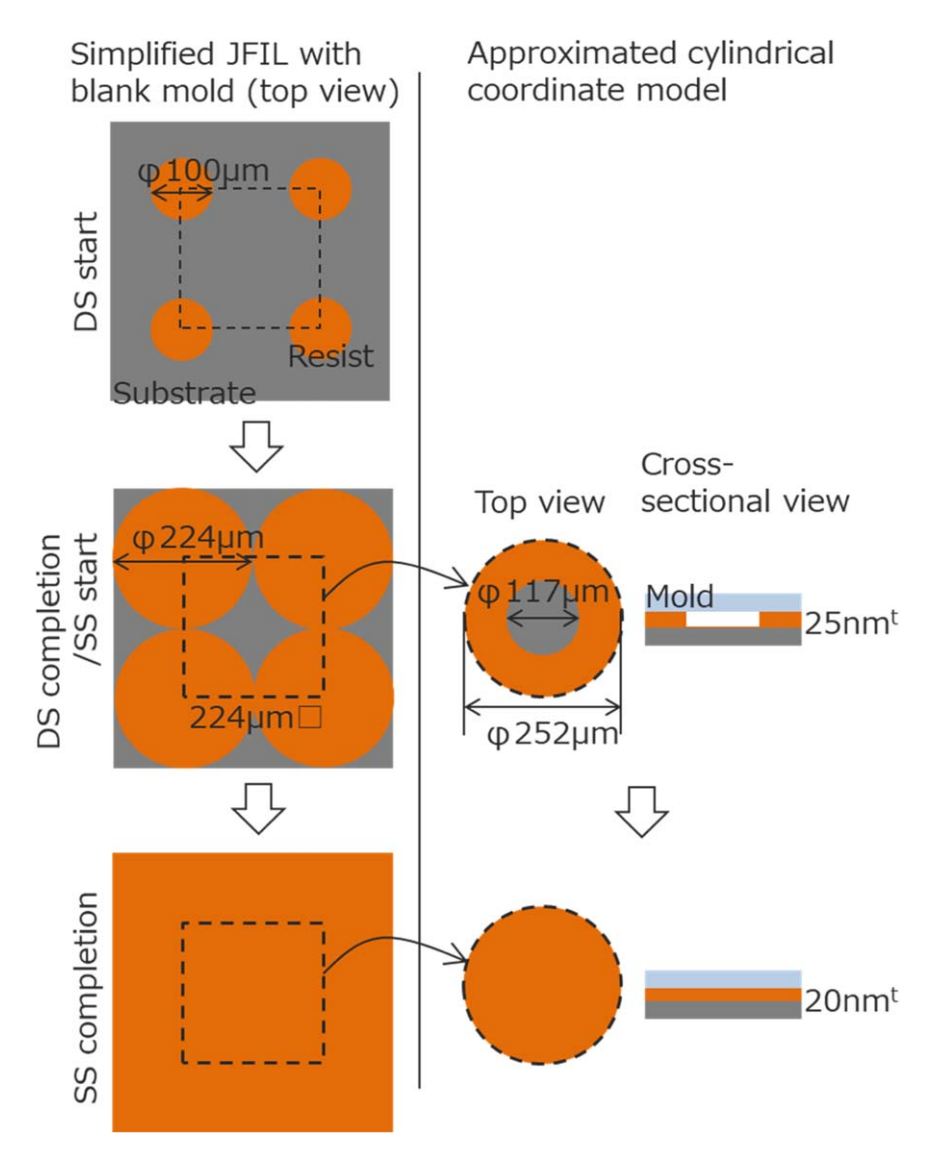


Fig. 7. Calculation model for DS and SS.

The gas disappearance behavior can be described by a four-step loop. A theoretical calculation loop of the gas diffusion in SS is shown in Fig. 8.

Firstly, trapped ambient gas is compressed by the Laplace pressure generated at the interface along the mold, the substrate, and the resist. Laplace pressure is calculated based on the Young–Laplace equation. ²⁴⁾ The equation of state of ideal gas and the equation of mass of gas are also taken into the calculation.

Secondly, the trapped gas permeates into each layer by being pushed by the Laplace pressure. Gas permeation behavior is described by the gas diffusion equation.²⁴⁾ Please refer to paper²⁴⁾ regarding the diffusion coefficients and the dissolution coefficients.

Thirdly, static liquid flow occurs to fill the loss volume of the gas bubble. The lubrication equation was solved to calculate the fluid flow of the resist liquid, assuming lubricant approximation. ²⁴⁾

Fourthly, the resist liquid is assumed to be non-condensable, so that the mold should be going down by being pulled down by the resist liquid. The equation of motion of the mold is solved.²⁴⁾

The gap distance between the mold and the substrate narrows, so that the Laplace pressure is updated with the new gap. All four steps described above are calculated repeatedly in this order until the completion of gas disappearance.

2.1.2. Experiment. JFIL resist was formulated with some acrylates and photo-initiators. ODL -301 provided by Shin-Etsu Chemical Industry Co. Ltd. was used as the spin-on carbon (SOC).

Drops of 1 pL of resist in a square array of 140 μ m per side were uniformly dropped in a range on a field size 26 \times 33 mm on a silicon substrate or on a silicon substrate coated with the SOC having a thickness of 200 nm, and a quartz blank mold was brought into contact with the droplets.

The number of trapped gas bubbles during various imprinting times was measured using a defect inspection tool 2905LP provided by KLA Tencor.

2.1.3. Results and discussion. In the case where the thickness of the resist liquid film is thinner than 100 nm, the gas disappearance time of CO₂ gas is faster than that of helium gas on a silicon substrate. The relationship between imprinting time and defect density in JFIL with a resist film 500 nm thick on a silicon substrate is shown in Fig. 9.

CO₂ ambient gas showed a lower defect density in a shorter imprinting time; that is, the gas disappearance time is faster in CO₂ ambient gas than helium ambient gas.

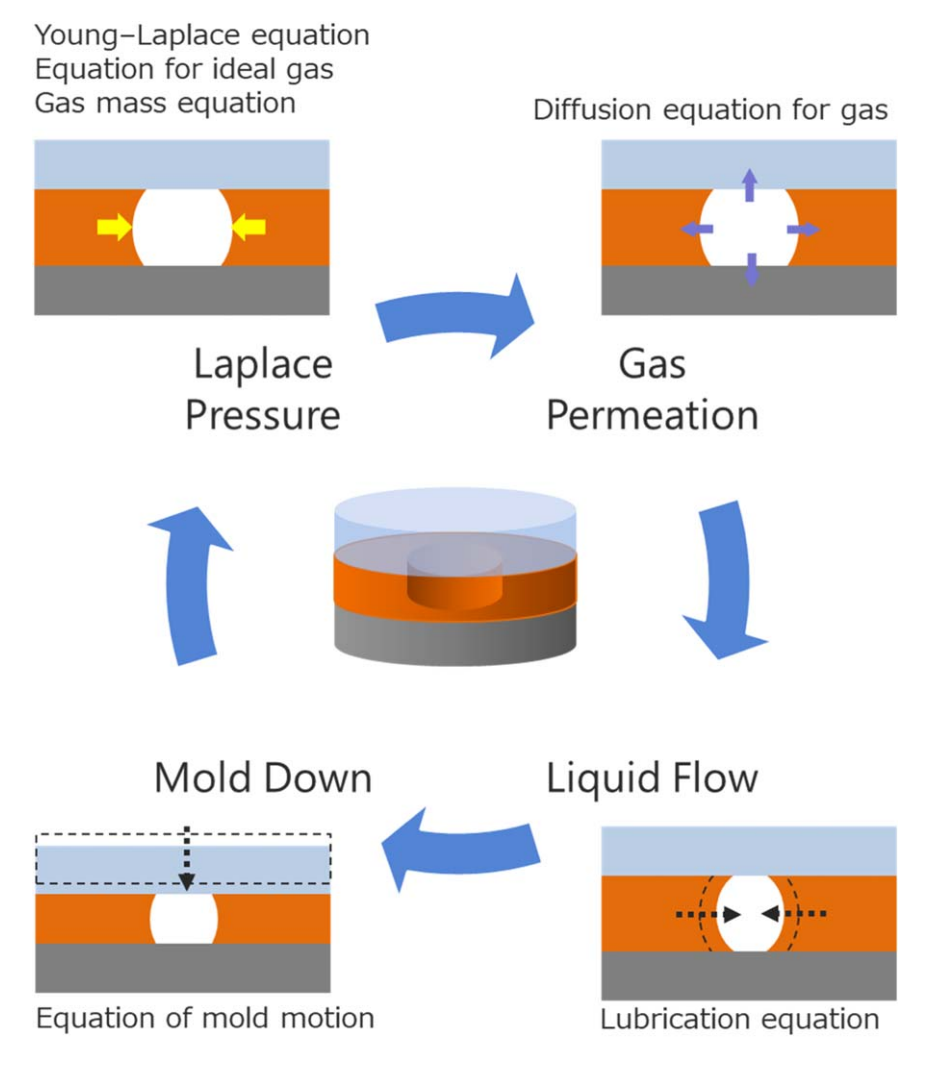


Fig. 8. Theoretical calculation loop of gas diffusion in SS.

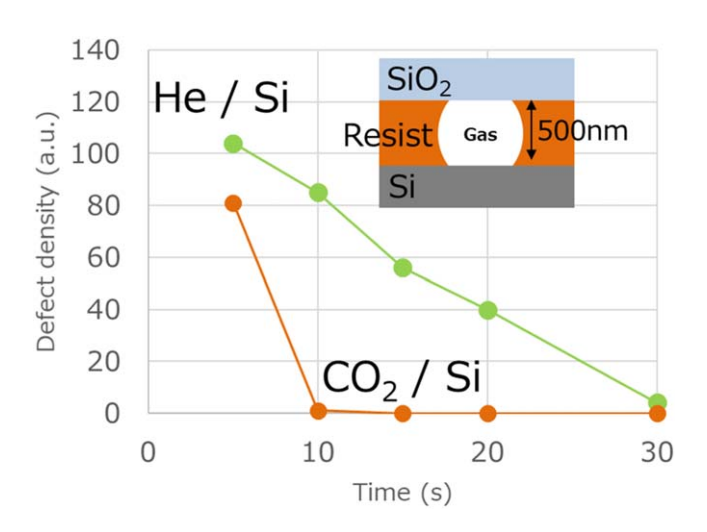


Fig. 9. Defect density on a silicon substrate.

In the actual lithography process of semiconductor device manufacturing, an organic solid layer such as SOC is often applied as an underlayer.²⁹⁾ In the case that the SOC layer is applied on a silicon wafer as an underlayer in JFIL, it was calculated that the gas disappearance time is faster in a SOC/ silicon substrate than a silicon substrate, since helium gas can diffuse into the SOC and CO₂ gas can dissolve into the SOC.²⁵⁾ The calculated gas disappearance time on silicon

wafers coated with SOC $0\sim200\,\mathrm{nm}$ thick is plotted in Fig. 10.

On SOC film 0 nm thick—that is, on a bare silicon substrate—helium gas disappeared the fastest. This was considered to be because of the fast diffusion of helium gas into the quartz mold. However, on SOC film thicker than 5 nm, CO₂ gas disappeared the fastest. This was considered to be because of the fast dissolution of CO₂ gas into the SOC film.

The JFIL experiment was carried out on a silicon wafer coated with SOC 200 nm thick. The relationship between imprinting time and defect density is plotted in Fig. 11.

In ambient gas of both helium and CO₂, the defect densities on the SOC-coated silicon wafer were less than the result obtained on a bare silicon wafer, shown in Fig. 10. The permeability of all the gas molecules to the organic layer is considered higher than those to silicon crystalline. Especially in a short imprinting time of 0.7~0.9 s, CO₂ ambient gas showed less defect density than helium ambient gas.

2.2. Combined-drop JFIL

In spite of the effort described in the previous section, it has still been difficult to eliminate the bubbles perfectly and quickly.³⁰⁾ For the purpose of further reduced volume of trapped ambient gas, a novel JFIL process and resist material have been developed.

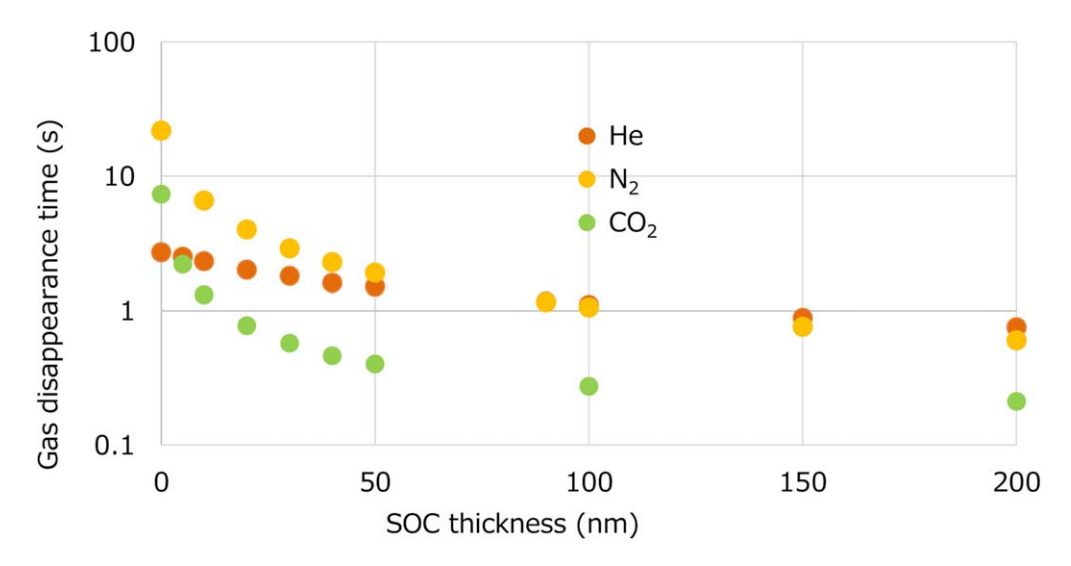


Fig. 10. SOC thickness and gas disappearance time.

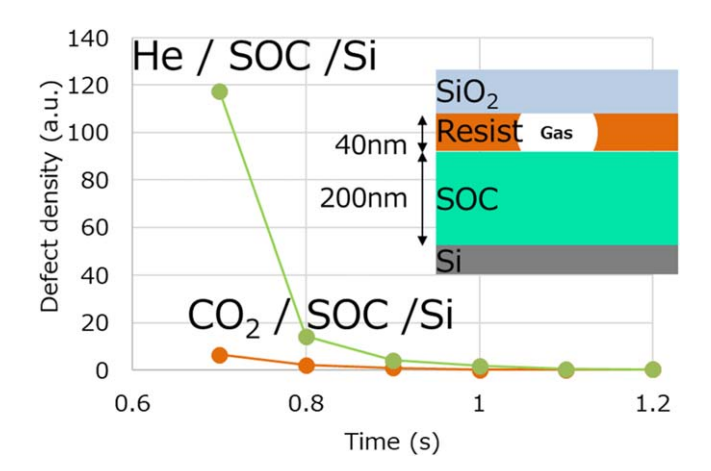


Fig. 11. Defect density on a SOC-coated silicon wafer.

We considered that drops of imprint resist should spread widely and should combine to adjacent drops prior to imprinting. Fluid-control technology of the drop liquid was developed based on fluid mechanics, interface science, and liquid property design to ensure the imprint resist drops quickly expanded and combined with each other prior to imprinting (Fig. 12); this technology was named combined-drop JFIL (CD-JFIL). In CD-JFIL, the trapped gas volume is minimized to reduce the imprint time and bubble defects.³¹⁾

In conventional JFIL, dispensed drops of 1pL spread to about 100 μ m diameter and then stop; then, the mold contacts

the resist drops. On the other hand, a resist composition that can spread fast and widely is used in CD-JFIL to ensure the resist drops form a continuous liquid film. In addition, drop height is also reduced to get the gap between the mold and the substrate low when the mold contacts the resist film, which results in less volume of ambient gas being trapped between the mold and the substrate.

2.2.1. Calculation. Liquid drops of 1 pL were arranged in a square array on a flat substrate with an initial contact angle of 90°; the solvent in the drops spread while volatilizing to form a continuous liquid film, which was obtained by solving the Navier–Stokes equation in the thin film approximation (lubrication theory) with a free surface.

2.2.2. Experiment. The JFIL resist was formulated with some acrylates and photo-initiators. The CD-JFIL resist was prepared by diluting the JFIL resist of 20 vol% with a solvent of 80 vol%.

The drop-spreading behavior was observed using an inkjet apparatus capable of dispensing 1pL droplets. A nanoimprint tool prototyped by Canon was used for the imprinting test. The imprinted films were observed under a microscope and inspected for defects using a defect inspection tool 2905LP provided by KLA Tencor.

2.2.3. Results and discussion. Figure 13 shows the theoretical calculation result of the spreading behavior of the dispensed drops. In CD-JFIL, the drops started to combine with each other after 0.3 s, and a completely continuous liquid film was formed almost at the same time

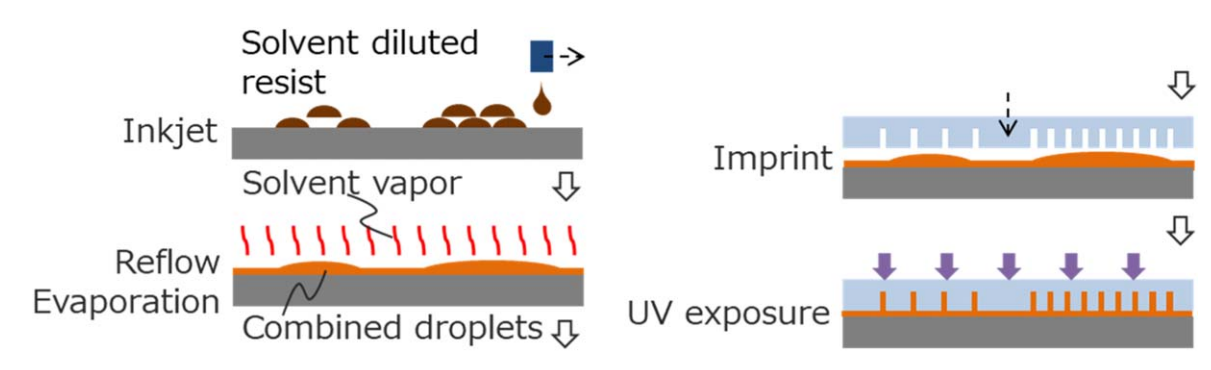


Fig. 12. Combined-drop JFIL (CD-JFIL).

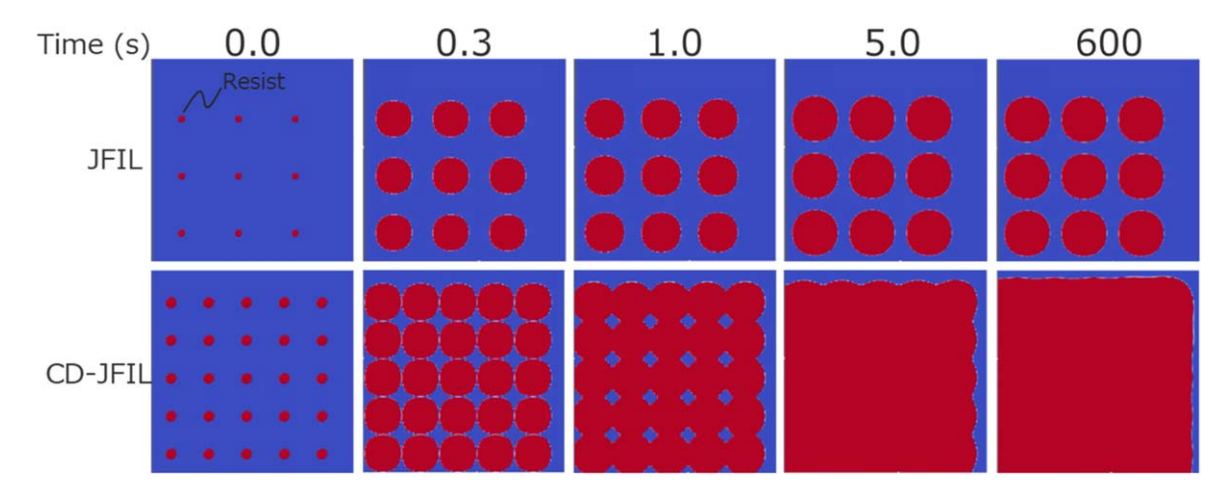


Fig. 13. Theoretical calculation of drop expansion (top view).

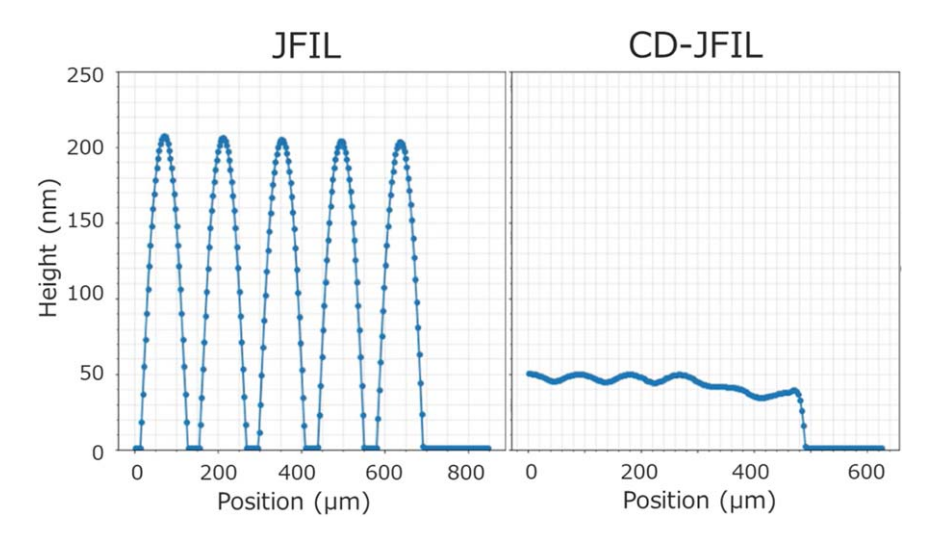


Fig. 14. Cross-sectional view of theoretically calculated drops 112 s after being dispensed.

as the volatilization was completed 4 s after dispensing. In the conventional JFIL resist system, the droplets were not combined even after 600 s.

The drop height is also obtained with the theoretical calculation. A cross-sectional view of drops 112 s after dispensing is shown in Fig. 14. While the drops are still independent and the liquid drop height is still higher than 200 nm in JFIL, the height of continuous liquid film in CD-JFIL is around 50 nm. In the other words, the gaps between the mold and the substrate at the moment of mold contact is about 200 nm and 50 nm in JFIL and CD-JFIL, respectively. This result means that the total gas volume trapped between the mold and the substrate is smaller in CD-JFIL than in JFIL.

Figure 15 shows the droplet-spreading behavior of the CD-JFIL resist observed on an inkjet station. In general agreement with the theoretical calculation, the combination of the liquid film was completed in about 5 s, and the liquid film was planarized in about 30 s.

After the volatilization of the solvent was completed, a blank mold made of quartz was imprinted, and 0.7 s after the imprinting, the resist liquid film was observed through the mold under a microscope (Fig. 16). In the conventional JFIL resist system, the ambient gas was trapped between the drops and hardly disappeared, while in the CD-JFIL, it was almost zero.

Figure 17 shows the results of measuring the number of bubbles larger than 26 nm in diameter at each imprinting time

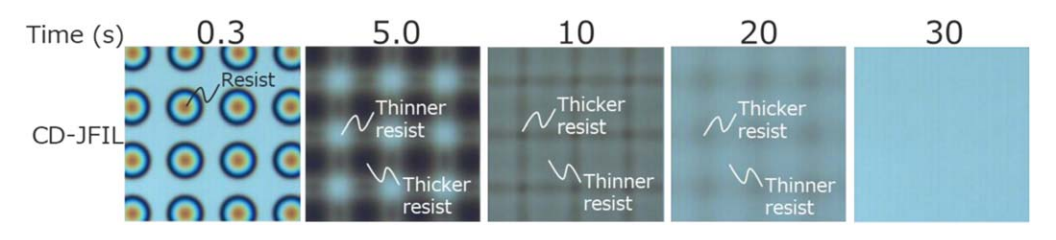


Fig. 15. Experimental result of drop expansion.

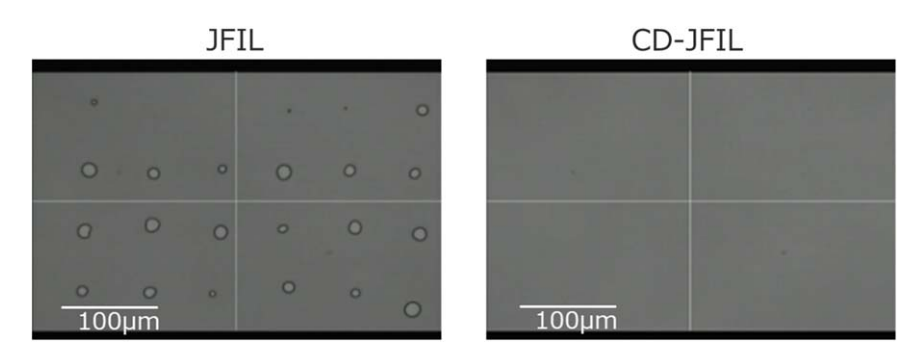


Fig. 16. Trapped bubbles 0.7 s after imprinting.

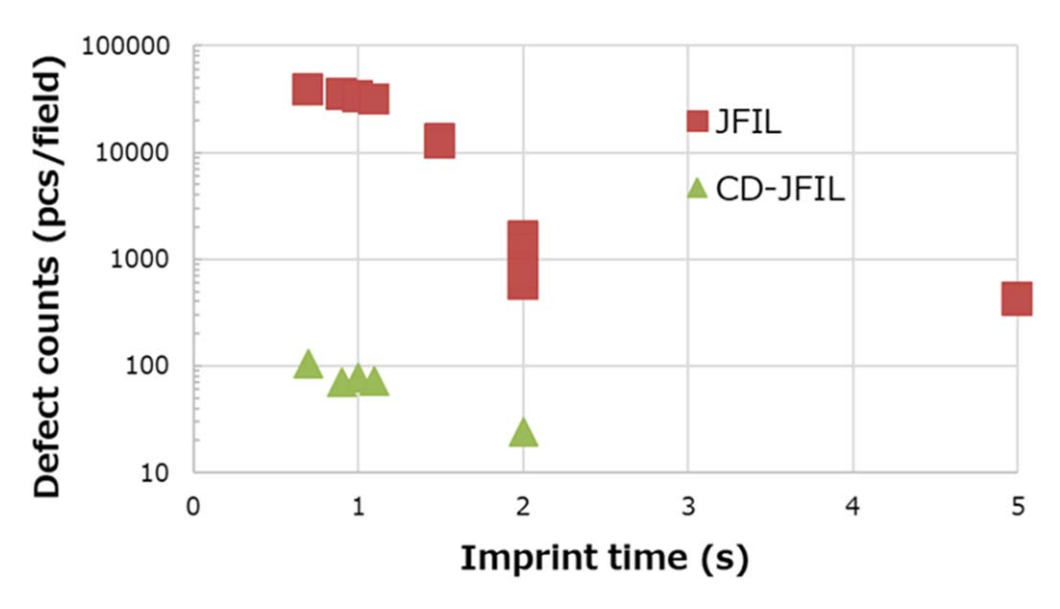


Fig. 17. Defect counts and imprint time.



 $\textbf{Fig. 18.} \quad \text{Nanoimprint semiconductor manufacturing equipment FPA-} \\ 1200NZ2C.$

in the imprint field of 26×33 mm by the defect inspection tool 2905LP.

In conventional JFIL, there were tens of thousands of particles with an imprinting time of 0.7 s; the trapped gas gradually diffused into the quartz, and the bubbles gradually disappeared, still resulting in hundreds of particles even at 5 s. On the other hand, in the case of CD-JFIL, the number of bubbles was already less than 100 after 0.7 s of imprinting time.

3. Conclusions

CO₂ ambient gas and CD-JFIL reduced the ambient gas trapped in JFIL technology, which is expected to reduce non-fill defects and to improve throughput.

Nanoimprint equipment FPA-1200NZ2C (Fig. 18), developed by Canon, is being used in a semiconductor device company for trial manufacturing of memory devices.

NIL technology will be used to try to manufacture Not AND (NAND) flash memories, which allows a certain number of defects. Further effort will be made to reduce the defect number and foreign particles, and then it is expected to be possible to apply NIL on Dynamic Random Access Memory and logic devices that have less redundancy in the circuit design.

- S. Y. Chou, P. R. Krauss, and P. J. Renstrom, J. Vac. Sci. Technol. B 14, 4129 (1996)
- T. K. Whidden, D. K. Ferry, M. N. Kozicki, E. Kim, A. Kumar, J. Wilbur, and G. M. Whitesides, Nanotechnology 7, 447 (1996).
- 3) M. Colburn et al., Proc. SPIE 3676, 379 (1999).
- 4) T. C. Bailey et al., Microelectron. Eng. 461, 61 (2002).
- J. Choi, K. Nordquist, A. Cherala, L. Casoose, K. Gehoski, W. J. Dauksher,
 S. V. Sreenivasan, and D. J. Resnick, Microelectron. Eng. 633, V78 (2004).
- I. McMackin, J. Choi, P. Schumaker, V. Nguyen, F. Xu, E. Thompson, D. Babbs, S. V. Sreenivasan, M. Watts, and N. Schumaker, Proc. SPIE 5374, 222 (2004).
- 7) S. Reddy and R. T. Bonnecaze, Microelectron. Eng. 82, 60 (2005).
- 8) K. Selenidis, J. Maltabes, I. McMackin, J. Perez, W. Martin, D. J. Resnick, and S. V. Sreenivasan, Proc. SPIE 6730, 67300F-1 (2007).

- I. Yoneda, Y. Nakagawa, S. Mikami, H. Tokue, T. Ota, T. Koshiba, M. Ito, K. Hashimoto, T. Nakasugi, and T. Higashiki, Proc. SPIE 7271, 72712A (2009).
- T. Higashiki, T. Nakasugi, and I. Yoneda, Proc. SPIE 7970, 797003 (2011).
- 11) Z. Ye et al., Proc. SPIE 8680, 86800C (2013).
- 12) N. Khusnatdinov et al., Proc. SPIE 9049, 904910 (2014).
- 13) H. Takeishi and S. V. Sreenivasan, Proc. SPIE 9423, 94230C (2015).
- 14) T. Ito, K. Emoto, T. S. Takashima, K. Sakai, W. Liu, J. DeYoung, Z. Ye, and D. LaBrake, J. Photopolym. Sci. Tech. 29, 159 (2016).
- 15) W. Zhang et al., Proc. SPIE 9777, 97770A (2016).
- T. Takashima, Y. Takabayashi, N. Nishimura, K. Emoto, T. Matsumoto, T. Hayashi, A. Kimura, J. Choi, and P. Schumaker, Proc. SPIE 9777, 977706 (2016).
- 17) K. Emoto et al., Proc. SPIE 9777, 97770C (2016).
- 18) T. Iwanaga, Micro and Nano Engineering 2016 Scientific Program (2016).
- Z. Hamaya, J. Seki, T. Asano, K. Sakai, A. Aghili, M. Mizuno, J. Choi, and C. Jones, Proc. SPIE 10810, 108100F (2018).
- T. Ifuku, M. Hiura, Y. Takabayashi, A. Kimura, Y. Suzaki, T. Ito, K. Yamamoto, B. J. Choi, T. Estrada, and D. J. Resnick, Proc. SPIE 12293, 122930E (2022).
- H. Tanaka, N. Maruyama, M. Hiura, Y. Suzaki, A. Kimura, K. Yamamoto, T. Matsumoto, K. Yamamoto, and Y. Takabayashi, Proc. SPIE 12751, 127510D (2023).
- 22) B. H. Chao et al., Proc. SPIE 6921, 69210C (2008).
- H. Hiroshima, M. Nakagawa, Y. Hirai, and S. Matsui, J. Photopolym. Sci. Technol. 26, 87 (2013).
- 24) T. Ito, Y. Ito, I. Kawata, K-ichi Ueyama, K. Nagane, W. Liu, T. Stachowiak, W. Zhang, and T. Estrada, J. Photopolym. Sci. Tech. 35, 105 (2022).
- M. Khawaja, A. P. Sutton, and A. A. Mostofi, J. Phys. Chem. B 121, 287 (2017).
- 26) J. F. Shackelford, Procedia Mater. Sci. 7, 278 (2014).
- 27) I. M. McMackinNicholas, A. StaceyDaniel, A. BabbsDuane, J. VothMichael, P. C. Watts, V. N. Truskett, F. Y. Xu, R. D. Voisin, and P. B. Lad, US Patent 7090716 (2003).
- 28) T. Ito, Y. Ito, I. Kawata, K.-I. Ueyama, K. Nagane, W. Liu, T. Stachoviak, W. Zhang, and T. Estrada, 2022 Int. Symp. on Semiconductor Manufacturing, PO-62 (2022).
- 29) K. Okabe, T. Higuchi, M. Komori, and T. Kono, J. Micro/Nanopattern., Mater. Metrology 21, 011006 (2022).
- N. Khusnatdinov, T. Stachowiak, and W. Liu, Proc. SPIE 10584, 105840S (2018).
- T. Ito, J. Shirono, H. Matsushima, H. Imamura, T. Stachoviak, and W. Liu, International Workshop on Dielectric Thin Films for Future Electron Devices Science and Technology S1-4, 11 (2023).